IEEE Photonics Journal
An IEEE Photonics Society Publication

Open Access

High-Performance Semi-Polar InGaN/GaN Green Micro Light-Emitting Diodes

Volume 12, Number 1, February 2020

Fei-Fan Xu
Tao Tao
Bin Liu, *Senior Member, IEEE*
Xuan Wang
Mao-Gao Gong
Ting Zhi
Dan-Feng Pan
Zi-Li Xie
Yu-Gang Zhou, *Member, IEEE*
You-Dou Zheng
Rong Zhang

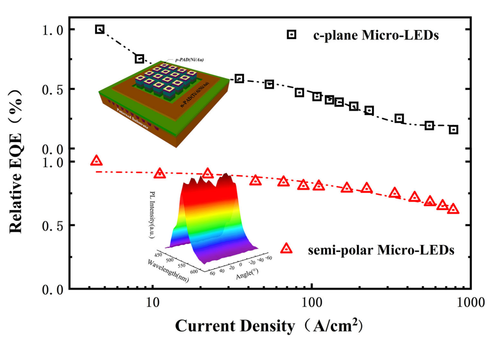

DOI: 10.1109/JPHOT.2019.2962184

IEEE photonics SOCIETY
IEEE

High-Performance Semi-Polar InGaN/GaN Green Micro Light-Emitting Diodes

Fei-Fan Xu,[1,2] Tao Tao,[1,2] Bin Liu ,[1,2] *Senior Member, IEEE*, Xuan Wang,[1,2] Mao-Gao Gong,[1,2] Ting Zhi,[3] Dan-Feng Pan,[1,2] Zi-Li Xie,[1,2] Yu-Gang Zhou ,[1,2] *Member, IEEE*, You-Dou Zheng,[1,2] and Rong Zhang[1,2,4]

[1]Key Laboratory of Advanced Photonic and Electronic Materials, School of Electronic Science and Engineering, Nanjing University, Nanjing, 210023, China
[2]Nanjing National Laboratory of Microstructures, Nanjing University, Nanjing, 210023, China
[3]College of Electronic and Optical Engineering & College of Microelectronics, Nanjing University of Posts and Telecommunications, Nanjing, 210023, China
[4]Xiamen University, Xiamen 316005, P. R. China

DOI:10.1109/JPHOT.2019.2962184

Manuscript received December 2, 2019; revised December 18, 2019; accepted December 21, 2019. Date of publication December 20, 2019; date of current version January 7, 2020. This work was supported in part by the National Key R&D Program of China under Grants 2017YFB0403100, 2017YFB0403101, in part by National Nature Science Foundation of China under Grants 61921005, 61674076, 61674081, 61605071, 61974062, in part by Nature Science Foundation of Jiangsu Province under Grants BY2013077, BK20141320, BE2015111, Six Talent Peaks Project of Jiangsu Province under Project XYDXX-081, Open Fund of the State Key Laboratory on Integrated Optoelectronics under Grant IOSKL2017KF03, Fundamental Research Funds for the Central Universities under Grant 021014380096, Collaborative Innovation Center of Solid State Lighting and Energy-saving Electronics.
Corresponding authors: Tao Tao; Bin Liu (e-mail: ttao@nju.edu.cn; bliu@nju.edu.cn).

Abstract: Semi-polar micro-LEDs have gain increasing interests due to the advantages of polarization control and quantum efficiency improvement. In this work, a novel semi-polar (20–21)-plane micro-LEDs array has been designed and manufactured. In comparison with c-plane micro-LEDs, semi-polar micro-LEDs indicate better electrical and optical performance. The relative EQE of semi-polar micro-LEDs remains at 62% under the injected current density of 775.6 A/cm^2, which indicates a reduced efficiency droop due to less polarization in MQWs. It has been further proved by a significant reduction of 55% in emission peak blue-shift under the injected current density from 11.1 A/cm^2 to 775.6 A/cm^2. In addition, the carrier recombination dynamics and spatial light distribution of semi-polar micro-LEDs with different pixel sizes have been studied. Fast recombination lifetime in smaller size semi-polar micro-LEDs indicates a promising way to be used as a high modulation bandwidth light source. Stable and uniform light distribution in a wider range of spatial azimuths further supports for the semi-polar micro-LEDs as a strong candidate for the applications of high-resolution display and high-speed visible light communication.

Index Terms: III-nitrides, semi-polar, micro-LEDs, InGaN/GaN, green.

1. Introduction

Micro-Leds have gained increasing interests in the field of high-resolution display and high speed visible light communication [1], [2]. Compared with standard millimeter-size LEDs, micro-LEDs have several advantages including smaller chip size, uniform current spread, lower power consumption, high efficiency and high photoelectric modulation bandwidth [3], [4]. Recently, some promising potential applications of micro-LEDs in many fields including high-resolution display, high-speed optical communication and optogenetics, etc have been reported. Full-color pixelated-addressable micro-LEDs on a transparent substrate have been fabricated by Lau et al [5]; By using atomic layer deposition and nonradiative resonant energy transfer, Kuo et al, have realized full-color monolithic hybrid quantum dot nanoring micro-LEDs very recently [6]. Dawson's research team has realized high speed visible light communications using individual pixels in micro-LEDs array, and a data transmission rate of 11.95 Gb/s has been achieved [1], [7]. Tian et al realized high-speed underwater optical wireless communication based on micro-LEDs [8]. For industry, Samsung released "The Wall" TV based on micro-LEDs technology in 2018; Meanwhile, Sony has introduced a 16k display device based on micro-LEDs technology in 2019. However, despite the great progress of micro-LEDs in academics and industry, some issues remain unsolved and limit the applications of micro-LEDs. Especially, the luminous peak blue-shift and efficiency droop are major problems that to be resolved urgently.

Conventional c-plane InGaN/GaN multiple quantum wells (MQWs) LED structures grown on c-plane sapphire substrates suffer strong polarization. Both piezoelectricity and spontaneous polarization exist in InGaN/GaN MQWs, leading to a severe quantum confined Stark effect (QCSE) [9], [10]. The QCSE might cause not only a significant peak shift but also great luminous efficiency droop under high injection current, which is believed as an important reason for the significant deterioration of the device performance, but other mechanisms such as Auger recombination and carrier leakage can also contribute to efficiency droop [9], [11], [12]. In recent years, impressive advancements in semi-polar nitride semiconductors and devices of visible light and deep-ultraviolet light emission have been achieved [13], which demonstrates that the polarization in InGaN/GaN MQWs could be effectively decreased by the construction of semi-polar orientation [14], [15]. Considering the benefits of semi-polar InGaN/GaN in high luminous efficiency, stable wavelengths of light [16], and extended the functionality in applications including high-resolution display, high-speed visible light communication and biomedicine, scientists started to devote their efforts to developing semi-polar GaN-based micro-LEDs. For instance, visible light communications, as a crucial role in communications, tactical surveillance and oceanography investigation, one key issue is to improve the modulation characteristics of LED light source and the emission performances under high-speed modulation [17]. It has been widely reported that the modulation characteristics of LED mainly depend on the following two aspects: RC time and carrier recombination lifetime. Obviously, LED devices with larger active area will limit the modulation bandwidth [18], [19]. Micro-LED with smaller pixel size could reduce RC time, and semi-polar InGaN/GaN MQWs with less QCSE could have faster radiative recombination, thus semi-polar micro-LEDs provide a potential candidate for improving the modulation characteristics for visible light communication applications.

However, there are few reports about the micro-LEDs based on semi-polar InGaN/GaN MQWs up to now. In this work, (20–21)-plane semi-polar micro-LEDs structures were designed and fabricated for the first time, whose electrical and optical properties are analyzed and compared with conventional c-plane micro-LEDs. In addition, the carrier recombination dynamics and spatial light distribution of semi-polar micro-LEDs with different sizes have been studied for the sake of achieving high-resolution display and high-speed modulation, which hold a huge potential for fast visible light communication.

2. Experiment

The three-dimensional (3D) structural and SEM images of semi-polar and c-plane green micro-LEDs are illustrated in Fig. 1. The LED sample is grown on a 2-inch sapphire substrate by metal-organic chemical vapor deposition (MOCVD), which consists of 3 μm undoped GaN buffer layer, a 2 μm Si-doped n-type GaN layer, a 10 period InGaN/GaN (3 nm/12 nm of c-plane and 4 nm/10 nm of semi-polar) multi-quantum wells (MQWs), and a 300 nm Mg-doped p-type GaN layer. The In content in InxGa1-xN layer of MQWs is designed to be about 0.4 for the sake of green light emission. The micron-pillar pixel areas were defined by photolithography and inductively coupled plasma (ICP) etching techniques using SiO_2 mask, where the etching depth is 1.2 μm. The sidewall

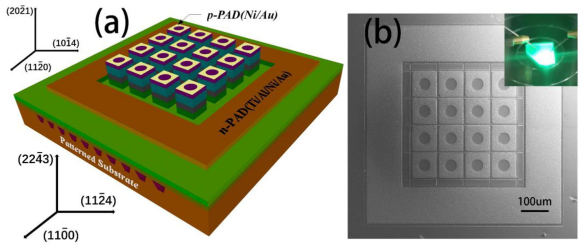

Fig. 1. (a) 3D schematic diagram and crystal orientation of semi-polar micro-LEDs samples on pattern sapphire substrates; (b) SEM image of semi-polar micro-LEDs array, Inset: Photo of luminescence under the injection current of 0.1 mA.

was passivated by a 200-nm-thick SiO_2 layer deposited by plasma enhanced chemical vapor deposition (PECVD) for reducing leakage channels and protecting devices after the wet chemical surface treatments involving the utilizing of potassium hydroxide (KOH) and nitric acid (HNO_3). Each pixel has an independent p-type contact pad (Ni: 30 nm/Au: 150 nm) with 50 μm diameter exposed circular window for light extraction. The p-type electrodes were annealed at 570 °C for 5 min to form Ohmic contact in a mixed atmosphere (80% nitrogen and 20% oxygen). All of the pixels in one unit share a common N-type electrode (Ti: 30 nm/Al: 150 nm/Ni: 50 nm/Au: 100 nm) and annealed at 750 °C in a nitrogen atmosphere for 30 s. As shown by the SEM image in Fig. 1(a) and (b), each pixel is separated by 5 μm wide deep trench to prevent cross-talk. The emission of a single micro-LED pixel is demonstrated in the inset of Fig. 1(b) under the injection current of 0.1 mA. In the later experiments, the time-resolved micro-PL (μ-TRPL) measurements were conducted by the excitation of pulsed laser source centered at 375 nm which was driven by the Pico Quant PDL800 picosecond pulsed lasers and detection with the single-photon sensitive detector (TCSPC system), and the beam size focused on the sample was about 3 μm. Then, angle-resolved excitation spectra were acquired using an angle-resolved microscope system (ARM17, Ideaoptics, Shanhai, China).

3. Results and Discussion

Room temperature electroluminescence (EL) spectra of c-plane and semi-polar micro-LEDs samples were measured under the injection current density ranging from 11.1 A/cm^2 to 775.6 A/cm^2. As illustrated in Fig. 2(a) and (b), the c-plane micro-LEDs sample exhibits a blue-shift from 526.3 nm to 511 nm, meanwhile, the semi-polar micro-LED sample has a relatively smaller blue-shift from 508.6 nm to 501.7 nm. It can be roughly estimated that the EL peak drift of semi-polar micro-LEDs is greatly reduced by about 55% compared with that of c-plane micro-LEDs. Here, semi-polar micro-LEDs with less QCSE demonstrate a promising application potential due to its stable emission peak. Furthermore, the current-voltage (I-V) characteristics of the c-plane and semi-polar micro-LEDs samples are compared in the logarithmic coordinate system as shown in Fig. 2(c). The turn-on voltage of semi-polar micro-LED samples is estimated to be 2.4 V, slightly larger than the 2.1 V of c-plane micro-LEDs. And the series resistance of semi-polar micro-LEDs samples is about 8 kΩ, slightly larger than the 5kΩ of c-plane micro-LEDs. Furthermore, the leakage current of all samples is about 1 nA under the reversed bias of -5 V, which is close to that of a standard planar LED [20], indicating a good electrical characteristic. Low leakage current leads to low device loss, which coincides with the concept of green environmental protection. The relative external quantum efficiency (EQE) of c-plane and semi-polar micro-LED samples is estimated with respect to the increasing current density. As the injected current density increased from 11.1 A/cm^2 to 775.6 A/cm^2, the relative EQE of semi-polar micro-LEDs decreased to 62% as shown in Fig. 2(d). In contrast, the relative EQE of the c-plane micro-LEDs decreased down to 16%, which might be mainly attributed to polarization induced QCSE, current overflow, and low injection efficiency

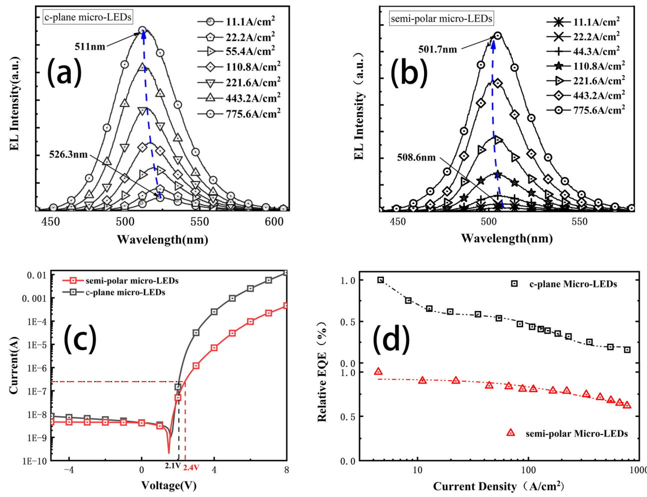

Fig. 2. (a) and (b) EL spectra under different current injection; (c) I-V characteristics of one pixel in the polar and semi-polar micro-LED; (d) normalized external quantum efficiency of one pixel in the polar and semi-polar micro-LED as a function of the injection current density, the fitting curves are plotted in dashed lines.

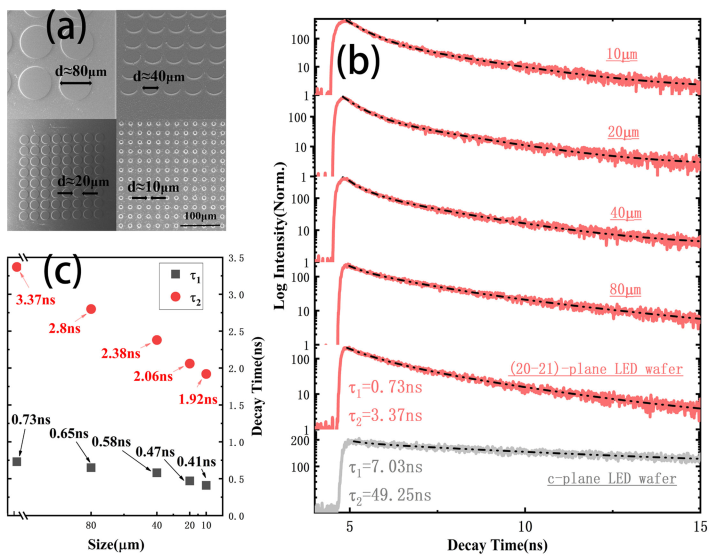

Fig. 3. (a) SEM images of micro-LEDs array with different sizes; (b) TRPL trace of c-plane and semi-polar micro-LED array structures with different sizes, the fitting results are plotted in dashed lines; (c) fast and slow decay time with respect to pixel size.

[21], [22]. Clearly, the semi-polar micro-LEDs with less efficiency droop in comparison with that of c-plane micro-LEDs further demonstrate the benefits from reduced QCSE by applying semi-polar structure.

For the sake of achieving high-resolution display and high-speed visible light communication, the size of each pixel in micro-LEDs should be as small as possible [23]. In this work, the micro-LEDs array with four different pixel sizes were designed and manufactured. As shown in Fig. 3(a), the diameters of the pixel area are 80 μm, 40 μm, 20 μm, and 10 μm, respectively. To understand the relationship of carrier recombination dynamics with respect to the pixel size in semi-polar micro-LEDs, room-temperature time-resolved micro-PL (μ-TRPL) measurements were performed. As demonstrated in Fig. 3(b), the TRPL traces of semi-polar micro-LED show a considerably faster initial decay than that of the conventional c-plane LED. A standard two exponential component

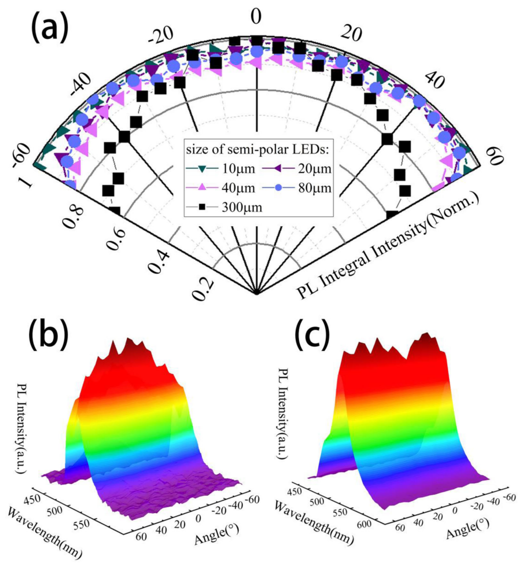

Fig. 4. (a) Normalized angular distribution of PL integral intensity from −60° to 60° of semi-polar LEDs with different sizes; (b) and (c) spatial light intensity release of semi-polar Micro-LED with a diameter of 300 μm and 80 μm.

model is used to study excitonic dynamics, and thus TRPL traces [I(t)] can be described by [24]–[26]

$$I(\mathrm{t}) = A_1 \exp\left(-\frac{t}{\tau_1}\right) + A_2 \exp\left(-\frac{t}{\tau_2}\right)$$

Where A_1 and τ_1 (A_2 and τ_2) are the fast (slow) decay components, both of which include radiative and nonradiative recombination [27]. Here, the fast and slow decay time of semi-polar (20–21)-plane green LED wafer were estimated to be 0.73 ns and 3.37 ns respectively, which are significantly shorter than the value of the c-plane LED wafer (7.03 ns and 49.25 ns). It further confirms that the reduced polarization in semi-polar InGaN/GaN MQWs could promote the recombination rate, therefore, resulting in an enhanced modulation bandwidth. Thus, semi-polar based micro-LEDs can be considered as a promising choice for visible light communication due to its much shorter carrier lifetime. As illustrated in Fig. 3(b), the TRPL traces are getting faster with respect to the decreasing size. The fast decay time is reduced from 0.65 ns to 0.41 ns as the diameter of micro-LEDs pixel decrease from 80 μm to 10 μm as shown in Fig. 3(c). Meantime, the slow decay time exhibits a larger reduction from 2.8 ns to 1.92 ns. It indicates that micro-LEDs with smaller pixels could have faster modulation speed. It should be mentioned that the RC time of LED is vital for visible light communication, could also be greatly reduced by shrinking the device size. It can be estimated that the modulation bandwidth of semi-polar micro-LEDs could be more than one order of magnitude higher than that about 500–600 MHz of c-plane green micro-LEDs according to published articles [1], [28]. Thus, the semi-polar based micro-LEDs array with smaller pixel size holds a huge potential for fast visible light communication as well.

Angular distribution of light sources is one important fact for visible light communication, which could affect the bit error rate and effective transmission range in the signal transmission [29]. In this work, normalized angular distribution measurements of PL integral intensity ranging from −60° to 60° have been conducted for semi-polar micro-LEDs with different sizes (80 μm, 40 μm, 20 μm, 10 μm) and semi-polar conventional planar LED (300μm). As shown in Fig. 4(a), the semi-polar micro-LEDs exhibit a much more uniform spatial intensity distribution from −60° to 60°, where the relative PL integral intensity remains above 0.8 when the diameter of the micro-LEDs is 80 μm. It can be seen that micro-LEDs have a wider emission angle compare with conventional planar LED, where more light can be extracted over a wider range of spatial azimuths, resulting in high light extraction efficiency. Meantime, with the size decreasing, the emission of micro-LEDs exhibits a more uniform spatial intensity distribution. Especially when the size of semi-polar micro-LEDs is decreased to 10 μm, the relative PL integral intensity remains more than 0.9. It demonstrates that smaller semi-polar micro-LEDs could have uniform spatial intensity distribution of emission, which is certainly beneficial for wide-angle transmission with high accuracy. The study of semi-polar micro-LEDs in this work could further promote the applications of high-speed micro-LED in visible light communication, and this provides a new way to reduce communication costs.

4. Conclusion

In conclusion, the semi-polar micro-LEDs array has been successfully designed and manufactured. Semi-polar micro-LEDs exhibit a good electrical and optical performance compared with c-plane micro-LEDs. A significant reduction in the efficiency droop and luminous peak blue-shift of semi-polar micro-LEDs has been observed. In addition, semi-polar micro-LEDs with smaller pixel sizes show faster carrier recombination lifetime, which is important for modulation bandwidth. And much more stable and uniform light distribution observed in spatial azimuths of semi-polar micro-LEDs demonstrate its potential for wide-angle transmission with high accuracy. Thus, semi-polar micro-LEDs become a promising candidate for many new applications including high-resolution display and high-speed visible light communication.

References

[1] M. S. Islim *et al.*, "Towards 10 Gb/s orthogonal frequency division multiplexing-based visible light communication using a GaN violet micro-LED," *Photon. Res.*, vol. 5, no. 2, pp. A35–A43, Apr. 1 2017.

[2] L. Zhu, C. W. Ng, N. Wong, K. K. Y. Wong, P. T. Lai, and H. W. Choi, "Pixel-to-pixel fiber-coupled emissive micro-light-emitting diode arrays," *IEEE Photon. J.*, vol. 1, no. 1, pp. 1–8, Jun. 2009.

[3] X.-H. Li, R. Song, Y.-K. Ee, P. Kumnorkaew, J. F. Gilchrist, and N. Tansu, "Light extraction efficiency and radiation patterns of III-nitride light-emitting diodes with colloidal microlens arrays with various aspect ratios," *IEEE Photon. J.*, vol. 3, no. 3, pp. 489–499, Jun 2011.

[4] J. Li *et al.*, "Advances and prospects in nitrides based light-emitting-diodes," *J. Semiconductors*, vol. 37, no. 6, Jun. 2016, Art. no. Unsp 061001.

[5] D. Peng, K. Zhang, V. S.-D. Chao, W. Mo, K. M. Lau, and Z. Liu, "Full-color pixelated-addressable light emitting diode on transparent substrate (LEDoTS) micro-displays by CoB," *J. Display Technol.*, vol. 12, no. 7, pp. 742–746, Jul. 2016.

[6] S.-W. H. Chen *et al.*, "Full-color monolithic hybrid quantum dot nanoring micro light-emitting diodes with improved efficiency using atomic layer deposition and nonradiative resonant energy transfer," *Photon. Res.*, vol. 7, no. 4, pp. 416–422, Apr. 1 2019.

[7] J. J. D. McKendry *et al.*, "High-speed visible light communications using individual pixels in a micro light-emitting diode array," *IEEE Photon. Technol. Lett.*, vol. 22, no. 18, pp. 1346–1348, Sep. 15 2010.

[8] P. Tian *et al.*, "High-speed underwater optical wireless communication using a blue GaN-based micro-LED," *Opt. Exp.*, vol. 25, no. 2, pp. 1193–1201, Jan. 23 2017.

[9] S. De *et al.*, "Quantum-confined stark effect in localized luminescent centers within InGaN/GaN quantum-well based light emitting diodes," *Appl. Phys. Lett.*, vol. 101, no. 12, Sep. 17 2012, Art. no. 121919.

[10] J.-H. Ryou *et al.*, "Control of quantum-confined stark effect in InGaN-based quantum wells," *IEEE J. Sel. Topics Quantum Electron.*, vol. 15, no. 4, pp. 1080–1091, Jul.-Aug. 2009.

[11] J. Piprek, "Efficiency droop in nitride-based light-emitting diodes," *Physica Status Solidi a-Appl. Mater. Sci.*, vol. 207, no. 10, pp. 2217–2225, Oct. 2010.

[12] Y. J. Zhao, H. Q. Fu, G. T. Wang, and S. Nakamura, "Toward ultimate efficiency: Progress and prospects on planar and 3D nanostructured nonpolar and semipolar InGaN light-emitting diodes," (in English), *Adv. Opt. Photon., Rev.*, vol. 10, no. 1, pp. 246–308, Mar 2018.

[13] R. G. Banal, Y. Taniyasu, and H. Yamamoto, "Deep-ultraviolet light emission properties of nonpolar M-plane AlGaN quantum wells," *Appl. Phys. Lett.*, vol. 105, no. 5, Aug. 4 2014, Art. no. 053104.

[14] Y. Enya *et al.*, "531 nm green lasing of InGaN based laser diodes on semi-polar {20(2)over-bar1} free-standing GaN substrates," *Appl. Phys. Express*, vol. 2, no. 8, Aug. 2009, Art. no. 082101.

[15] Y. Yoshizumi *et al.*, "Continuous-wave operation of 520 nm green InGaN-based laser diodes on semi-polar {20(2)over-bar1} GaN substrates," *Appl. Phys. Express*, vol. 2, no. 9, Sep. 2009, Art. no. 092101.

[16] M. Monavarian, A. Rashidi, and D. Feezell, "A decade of nonpolar and semipolar III-nitrides: A review of successes and challenges," *Physica Status Solidi a-Appl. Mater. Sci.*, vol. 216, no. 1, Jan. 9 2019, Art. no. 1800628.

[17] H. M. Oubei, C. Li, K.-H. Park, T. K. Ng, M.-S. Alouini, and B. S. Ooi, "2.3 Gbit/s underwater wireless optical communications using directly modulated 520 nm laser diode," *Opt. Exp.*, vol. 23, no. 16, pp. 20743–20748, Aug. 10 2015.

[18] J.-W. Shi, K.-L. Chi, J.-M. Wun, J. E. Bowers, Y.-H. Shih, and J.-K. Sheu, "III-nitride-based cyan light-emitting diodes with GHz bandwidth for high-speed visible light communication," *IEEE Electron Device Lett.*, vol. 37, no. 7, pp. 894–897, Jul. 2016.
[19] J.-M. Wun *et al.*, "GaN-based miniaturized cyan light-emitting diodes on a patterned sapphire substrate with improved fiber coupling for very high-speed plastic optical fiber communication," *IEEE Photon. J.*, vol. 4, no. 5, pp. 1520–1529, Oct. 2012.
[20] J.-H. Seo *et al.*, "A simplified method of making flexible blue LEDs on a plastic substrate," *IEEE Photon. J.*, vol. 7, no. 2, pp. 1–7, Apr. 2015, Art. no. 8200207.
[21] T. Lan, G. Zhou, Y. Li, C. Wang, and Z. Wang, "Mitigation of efficiency droop in an asymmetric GaN-based high-power laser diode with sandwiched GaN/InAlN/GaN lower quantum barrier," *IEEE Photon. J.*, vol. 10, no. 6, pp. 1–8, Dec. 2018, Art. no. 1504708.
[22] Z. Zhuang *et al.*, "Optical polarization characteristics of c-plane InGaN/GaN asymmetric nanostructures," *J. Appl. Phys.*, vol. 118, no. 23, Dec. 21 2015, Art. no. 233111.
[23] X. Liu *et al.*, "Gbps long-distance real-time visible light communications using a high-bandwidth GaN-based Micro-LED," *IEEE Photon. J.*, vol. 9, no. 6, pp. 1–9, Dec. 2017, Art. no. 7204909.
[24] S. F. Chichibu *et al.*, "Time-resolved photoluminescence, positron annihilation, and Al0.23Ga0.77N/GaN heterostructure growth studies on low defect density polar and nonpolar freestanding GaN substrates grown by hydride vapor phase epitaxy," *J. Appl. Phys.*, vol. 111, no. 10, May 15 2012, Art. no. 103518.
[25] J. H. Na *et al.*, "Dependence of carrier localization in InGaN/GaN multiple-quantum wells on well thickness," *Appl. Phys. Lett.*, vol. 89, no. 25, Dec. 18 2006, Art. no. 253120.
[26] S. Marcinkevicius, R. Ivanov, Y. Zhao, S. Nakamura, S. P. DenBaars, and J. S. Speck, "Highly polarized photoluminescence and its dynamics in semipolar (20(2)over-bar(1)over-bar) InGaN/GaN quantum well," *Appl. Phys. Lett.*, vol. 104, no. 11, Mar. 17 2014, Art. no. 111113.
[27] B. Liu, R. Smith, M. Athanasiou, X. Yu, J. Bai, and T. Wang, "Temporally and spatially resolved photoluminescence investigation of (11(2)over-bar2) semi-polar InGaN/GaN multiple quantum wells grown on nanorod templates," *Appl. Phys. Lett.*, vol. 105, no. 26, Dec. 29 2014, Art. no. 261103.
[28] C.-L. Liao, C.-L. Ho, Y.-F. Chang, C.-H. Wu, and M.-C. Wu, "High-speed light-emitting diodes emitting at 500 nm with 463-MHz modulation bandwidth," *IEEE Electron Device Lett.*, vol. 35, no. 5, pp. 563–565, May 2014.
[29] N. Sasaki, H. Shimada, S. Shimada, H. Kobayashi, and Ieee, "Evaluation of transmission quality of visible light communication using bit error rate measurement," in *Proc. 16th Int. Conf. Control, Autom. Syst. (Int. Conf. Control Autom. Syst.*, 2016, pp. 1362–1365.